16. Krijnen, P. A.; Nijmeijer, R.; Meijer, C. J.; Visser, C. A.; Hack, C. E.; Niessen, H. W. Apoptosis in myocardial ischaemia and infarction. J. Clin. Pathol. 55:801-811; 2002.

17. Kutschka, I.; Kofidis, T.; Chen, I. Y.; von Degenfeld, G.; Zwierzchoniewska, M.; Hoyt, G.; Arai, T.; Lebl, D. R.; Hendry, S. L.; Sheikh, A. Y.; Cooke, D. T.; Connolly, A.; Blau, H. M.; Gambhir, S. S.; Robbins, R. C. Adenoviral human BCL-2 transgene expression attenuates early donor cell death after cardiomyoblast transplantation into ischemic rat hearts. Circulation 114:I174-180; 2006.

18. Kuwana, T.; Newmeyer, D. D. Bcl-2-family proteins and the role of mitochondria in apoptosis. Curr. Opin. Cell Biol. 15:691-699; 2003.

19. Li, W.; Ma, N.; Ong, L. L.; Nesselmann, C.; Klopsch, C.; Ladilov, Y.; Furlani, D.; Piechaczek, C.; Moebius, J. M.; Lutzow, K.; Lendlein, A.; Stamm, C.; Li, R. K.; Steinhoff, G. Bcl-2 engineered MSCs inhibited apoptosis and improved heart function. Stem Cells 25:2118-2127; 2007.

20. Memon, I. A.; Sawa, Y.; Fukushima, N.; Matsumiya, G.; Miyagawa, S.; Taketani, S.; Sakakida, S. K.; Kondoh, H.; Aleshin, A. N.; Shimizu, T.; Okano, T.; Matsuda, H. Repair of impaired myocardium by means of implantation of engineered autologous myoblast sheets. J. Thorac. Cardiovasc. Surg. 130:1333-1341; 2005.

21. Naro, F.; Sette, C.; Vicini, E.; De Arcangelis, V.; Grange, M.; Conti, M.; Lagarde, M.; Molinaro, M.; Adamo, S.; Nemoz, G. Involvement of type 4 cAMP-phosphodiesterase in the myogenic differentiation of L6 cells. Mol. Biol. Cell 10:4355-4367; 1999.

22. Okano, T.; Yamada, N.; Okuhara, M.; Sakai, H.; Sakurai, Y. Mechanism of cell detachment from temperature-modulated, hydrophilic-hydrophobic polymer surfaces. Biomaterials 16:297-303; 1995.

23. Palojoki, E.; Saraste, A.; Eriksson, A.; Pulkki, K.; Kallajoki, M.; Voipio-Pulkki, L. M.; Tikkanen, I. Cardiomyocyte apoptosis and ventricular remodeling after myocardial infarction in rats. Am. J. Physiol. Heart Circ. Physiol. 280:H2726-2731; 2001.

24. Payne, T. R.; Oshima, H.; Okada, M.; Momoi, N.; Tobita, K.; Keller, B. B.; Peng, H.; Huard, J. A relationship between vascular endothelial growth factor, angiogenesis, and cardiac repair after muscle stem cell transplantation into ischemic hearts. J. Am. Coll. Cardiol. 50:1677-1684; 2007.

25. Perez-Ilzarbe, M.; Agbulut, O.; Pelacho, B.; Ciorba, C.; San Jose-Eneriz, E.; Desnos, M.; Hagege, A. A.; Aranda, P.; Andreu, E. J.; Menasche, P.; Prosper, F. Characterization of the paracrine effects of human skeletal myoblasts transplanted in infarcted myocardium. Eur. J. Heart Fail. 10:1065-1072; 2008.

26. Regula, K. M.; Ens, K.; Kirshenbaum, L. A. Mitochondria-assisted cell suicide: a license to kill. J. Mol. Cell. Cardiol. 35:559-567; 2003.

27. Saraste, A.; Pulkki, K.; Kallajoki, M.; Henriksen, K.; Parvinen, M.; Voipio-Pulkki, L. M. Apoptosis in human acute myocardial infarction. Circulation 95:320-323; 1997.

28. Scarabelli, T. M.; Gottlieb, R. A. Functional and clinical repercussions of myocyte apoptosis in the multifaceted damage by ischemia/reperfusion injury: old and new concepts after 10 years of contributions. Cell Death Differ. 11 Suppl 2:S144-152; 2004.

29. Seidel, M.; Borczynska, A.; Rozwadowska, N.; Kurpisz, M. Cell-based therapy for heart failure: skeletal myoblasts. Cell Transplant. 18:695-707; 2009.

30. Shimizu, S.; Konishi, A.; Kodama, T.; Tsujimoto, Y. BH4 domain of antiapoptotic Bcl-2 family members closes voltage-dependent anion channel and inhibits apoptotic

mitochondrial changes and cell death. Proc. Natl. Acad. Sci. U. S. A. 97:3100-3105; 2000.

31. Shimizu, T.; Yamato, M.; Isoi, Y.; Akutsu, T.; Setomaru, T.; Abe, K.; Kikuchi, A.; Umezu, M.; Okano, T. Fabrication of pulsatile cardiac tissue grafts using a novel 3-dimensional cell sheet manipulation technique and temperature-responsive cell culture surfaces. Circ. Res. 90:e40; 2002.

32. Umansky, S. R.; Tomei, L. D. Apoptosis in the heart. Adv. Pharmacol. 41:383-407; 1997.

33. Vaananen, A. J.; Salmenpera, P.; Hukkanen, M.; Rauhala, P.; Kankuri, E. Cathepsin B is a differentiation-resistant target for nitroxyl (HNO) in THP-1 monocyte/macrophages. Free Radic. Biol. Med. 41:120-131; 2006.

34. Vento, A.; Hammainen, P.; Patila, T.; Kankuri, E.; Harjula, A. Somatic stem cell transplantation for the failing heart. Scand. J. Surg. 96:131-139; 2007.

35. Yaffe, D. Retention of differentiation potentialities during prolonged cultivation of myogenic cells. Proc. Natl. Acad. Sci. U. S. A. 61:477-483; 1968.

36. Zhu, W.; Cowie, A.; Wasfy, G. W.; Penn, L. Z.; Leber, B.; Andrews, D. W. Bcl-2 mutants with restricted subcellular location reveal spatially distinct pathways for apoptosis in different cell types. EMBO J. 15:4130-4141; 1996.

TABLES

Table 1. Genes upregulated in Bcl-2-overexpressing L6 myoblast sheets as compared to wildtype cell sheets.

Gene name	*Fold change up*	*Description*
1372602_at	13.16	genethonin
1371126_x_at	8.017	granzyme B
1367782_at	7.712	cytochrome c oxidase, subunit VIa, polypeptide 2
1370694_at	6.571	tribbles homolog 3 (Drosophila)
1370464_at	6.491	ATP-binding cassette, sub-family B (MDR/TAP), member 1A
1369043_at	5.989	potassium voltage-gated channel, shaker-related subfamily, member 4
1397300_at	5.957	transcribed locus
1394681_at	5.947	aldo-keto reductase family 1, member C-like 1
1379402_at	5.815	ATP-binding cassette, sub-family C (CFTR/MRP), member 4
1386185_at	5.524	tripartite motif-containing 7
1368918_at	5.513	placental growth factor
1369772_at	5.027	solute carrier family 6 (neurotransmitter transporter, glycine), member 9
1373282_at	5.017	similar to mitochondrial carrier protein MGC4399
1389066_at	4.691	regulator of calcineurin 2
1369343_at	4.653	glutamate receptor interacting protein 1
1373807_at	2.244	vegf-A

Table 2. Echocardiography data at 3, 10, and 28 days after LAD-ligation and transplantation

3 days

	N	AWTd	PWTd	Dd	AWTs	PWTs	Ds	FS	EF
Sham	5	1.28±0.08	1.28±0.10	8.02±0.24	1.82±0.12	1.88±0.12	6.00±0.21	0.252±0.013	0.580±0.022
Control	22	1.18±0.04	1.45±0.04	8.18±1.13	1.21±0.04 †††	2.11±0.07	7.02±0.11 †††	0.140±0.012 †††	0.357±0.024 †††
L6-WT	17	1.08±0.06	1.45±0.05	7.84±0.18 *	1.06±0.06 †††,*	1.99±0.09	6.91±0.14 †††	0.116±0.010 †††	0.306±0.022 †††
L6-Bcl2	21	1.06±0.05 †,*	1.39±0.05	8.35±0.13 ‡	1.08±0.04 †††,*	2.07±0.07	7.34±0.14 †††,*,‡	0.121±0.010 †††	0.314±0.023 †††

10 days

	N	AWTd	PWTd	Dd	AWTs	PWTs	Ds	FS	EF
Sham	5	1.38±0.04	1.46±0.10	7.74±0.30	1.86±0.09	1.98±0.06	6.02±0.20	0.221±0.015	0.525±0.029
Control	22	0.58±0.03 †††	1.51±0.06	9.58±0.16 †††	0.58±0.03 †††	2.12±0.07	8.50±0.17 †††	0.114±0.008 †††	0.300±0.019 †††
L6-WT	17	0.59±0.04 †††	1.37±0.05 *	9.28±0.18 †††	0.65±0.05 †††	2.12±0.08	8.19±0.18 †††	0.114±0.010 †††	0.322±0.021 †††
L6-Bcl2	21	0.61±0.03 †††	1.44±0.06	9.44±0.17 †††	0.60±0.03 †††	2.33±0.08 †,*,‡	8.08±0.15 †††,*	0.144±0.010 †††,*,‡	0.378±0.019 †††,**,‡

28 days

	N	AWTd	PWTd	Dd	AWTs	PWTs	Ds	FS	EF
Sham	5	1.42±0.04	1.62±0.12	7.70±0.35	1.74±0.10	2.18±0.16	5.94±0.43	0.233±0.027	0.542±0.045
Control	22	0.60±0.03 †††	1.53±0.05	10.46±0.17 †††	0.61±0.03 †††	2.16±0.09	9.38±0.22 †††	0.106±0.008 †††	0.280±0.020 †††
L6-WT	17	0.55±0.04 †††	1.55±0.07	10.11±0.14 †††	0.52±0.04 †††,*	2.20±0.07	9.04±0.14 †††	0.106±0.006 †††	0.285±0.014 †††
L6-Bcl2	21	0.63±0.03 †††,‡	1.75±0.07 *,‡	10.61±0.17 †††	0.64±0.03 †††,‡	2.48±0.09 *,‡	9.27±0.18 †††	0.127±0.008 †††,*,‡	0.331±0.019 †††,*,‡

Values represent mean ± SEM

† $p<0.05$, ††† $p<0.001$ as compared to sham-operated group, * $p<0.05$ as compared to control group, ‡ $p<0.05$ as compared to L6-WT group

LEGENDS TO TABLES AND FIGURES

Table 1. Genes upregulated in Bcl-2-overexpressing L6 myoblast sheets as compared to wild type cell sheets.

Table 2. Echocardiography data at 3, 10, and 28 days after LAD ligation and transplantation showing anterior and posterior wall thickness in diastolic (AWTd, PWTd) and systolic phases (AWTs, PWTs) and left ventricular diameter in diastolic (Dd) and systolic (Ds) phases. Units are presented in mm. Dd and Ds were used to calculate fraction shortening (LVFS) and ejection fraction (LVEF) percentage.

Figure 1. Expressional and functional characterization of Bcl-2 in L6 myoblasts. A) Expression of Bcl-2 protein in wild type (L6-WT) and Bcl-2-overexpressing (L6-Bcl2) myoblasts. B) Immunofluorescence (IF) detection of Bcl-2 in L6 myoblasts suggesting cytoplasmic and perinuclear localization. C) Mitochondrial activity as measured with MTT assay in L6-WT and L6-Bcl2 in myoblast cultures treated for 48 hours. D) Number of adherent L6-WT and L6-Bcl2 myoblasts in cultures treated for 48 hours. E) Quantification of early apoptosis as measured by FITC-labeled annexin V binding to cell surface-translocated phosphatidyl serine. C-E) Cultures deprived of serum (left panels), and cultures with apoptosis induced by staurosporine (80 ng/ml) (right panels).

Figure 2. Immunohistochemistry, differentiation, and VEGF expression of wild type (L6-WT) and Bcl-2-overexpressing (L6-Bcl2) myoblast sheets. A) Hematoxylin and eosin (H&E) stain, expression of Bcl-2 protein, cell proliferation as detected by the expression of proliferation-associated Ki67 antigen and the evaluation of apoptotic cells by immunodetection for active cleaved caspase-3. B) Activation of caspase-3 in L6-WT and L6-Bcl2 myoblast sheets after 24 hours in control, serum-deprived, and staurosporine-treated (10 ng/ml) sheets. C) Immunoblots of myogenic differentiation markers troponin T and myogenin from L6-WT and L6-Bcl2 sheets after differentiation in serum-free medium for 96 hours. Lower panels show phase contrast images demonstrating the formation of myotubes in

L6-Bcl2 sheets. Cell detachment and death prevail in L6-WT sheets. D) Amount of VEGF-A in culture medium of untreated, serum-deprived, and staurosporine-treated L6-WT and L6-Bcl2 sheets as determined with ELISA.

Figure 3. Echocardiography for A) left ventricle ejection fraction (EF), and B) left ventricle fraction shortening at the indicated time points after wild type (n=17, L6-WT), Bcl-2-overexpressing (n=20, L6-Bcl2) myoblast sheet therapy for acute myocardial infarction (AMI). Control rats (n=22) underwent AMI without sheet transplantation, and sham-operated rats (n=5) underwent left-sided thoracotomy to control the surgery-induced effect on systolic parameters. * $p<0.05$, ** $p<0.01$ as compared to the control group; † $p<0.05$, †† $p<0.01$ as compared to the L6-WT group.

Figure 4. A) Quantitative evaluation of vascular density using immunohistochemical staining for von Willebrand factor (vWF) expression in myocardial paraffin-embedded sections from sham-operated, wild type (L6-WT), Bcl-2 (L6-Bcl2), and control animals. *$p<0.05$, ** $p<0.01$ as compared to the control group; † $p<0.05$, †† $p<0.01$ as compared to the L6-WT group. B) Expression of vWF in uninfarcted, sham-operated myocardium. C) Representative figures showing vascular density with vWF staining (brown) in infarct (left panels), border (middle panels), and remote (right panels) areas of the left ventricle. Sections were counterstained with hematoxylin (blue).

Figure 5. A) Quantitative evaluation of fibrosis by Sirius Red staining of myocardial paraffin-embedded sections from sham-operated, wild type (L6-WT), Bcl-2 (L6-Bcl2), and control animals. * $p<0.05$, ** $p<0.01$ as compared to the control group; † $p<0.05$, †† $p<0.01$ as compared to the L6-WT group. B) Background staining in uninfarcted, sham-operated myocardium. C) Representative figures showing the amount of fibrosis (red) in infarct (left panels), border (middle panels), and remote (right panels) areas of the left ventricle.

Figure 6. A) Quantitative evaluation of proliferative cells as assessed with the expression of proliferation associated Ki67 nuclear antigen (dark brown). Figure shows mean ± SEM densitometry values from the immunohistochemistry of myocardial paraffin-embedded

sections of sham-operated, wild type (L6-WT), Bcl-2 (L6-Bcl2), and control animals. * $p<0.05$, ** $p<0.01$ as compared to the control group, † $p<0.05$, †† $p<0.01$ as compared to the L6-WT group. B) Expression of Ki67 in uninfarcted, sham-operated myocardium. C) Representative figures of showing proliferating cells by Ki67 expression in infarct (left panels), border (middle panels), and remote (right panels) areas of the left ventricle. Sections were double-stained to detect muscle tissue by tropomyosin (red) expression. Sections were counterstained with hematoxylin (blue).

Figure 7. A) Quantitative evaluation of the number of c-kit expressing cells in the myocardium. Paraffin-embedded sections were stained from sham-operated, wild type (L6-WT), Bcl-2 (L6-Bcl2), and control animals. * $p<0.05$, as compared to the L6-WT group, ** $p<0.01$ as compared to the control group. B) Representative figures of c-kit expressing cells in the myocardium from sham-operated (upper left panel), control (upper right panel), L6-WT (lower left panel) and L6-Bcl2 (lower right panel) groups. Sections were counterstained with Nuclear Fast Red.

Figure 8. Quantitative evaluation of cell survival after myoblast cell sheet transplantation. A) Analysis of green fluorescence intensity from the apical surface of hearts 3 weeks after transplantation of GFP-expressing wild type (L6-WT-GFP, n=6) and Bcl-2-overexpressing (L6-Bcl2-GFP, n=6) cell sheets. B) Representative bright field (left panels) or fluorescence (right panels) images of excised hearts three weeks after surgery.

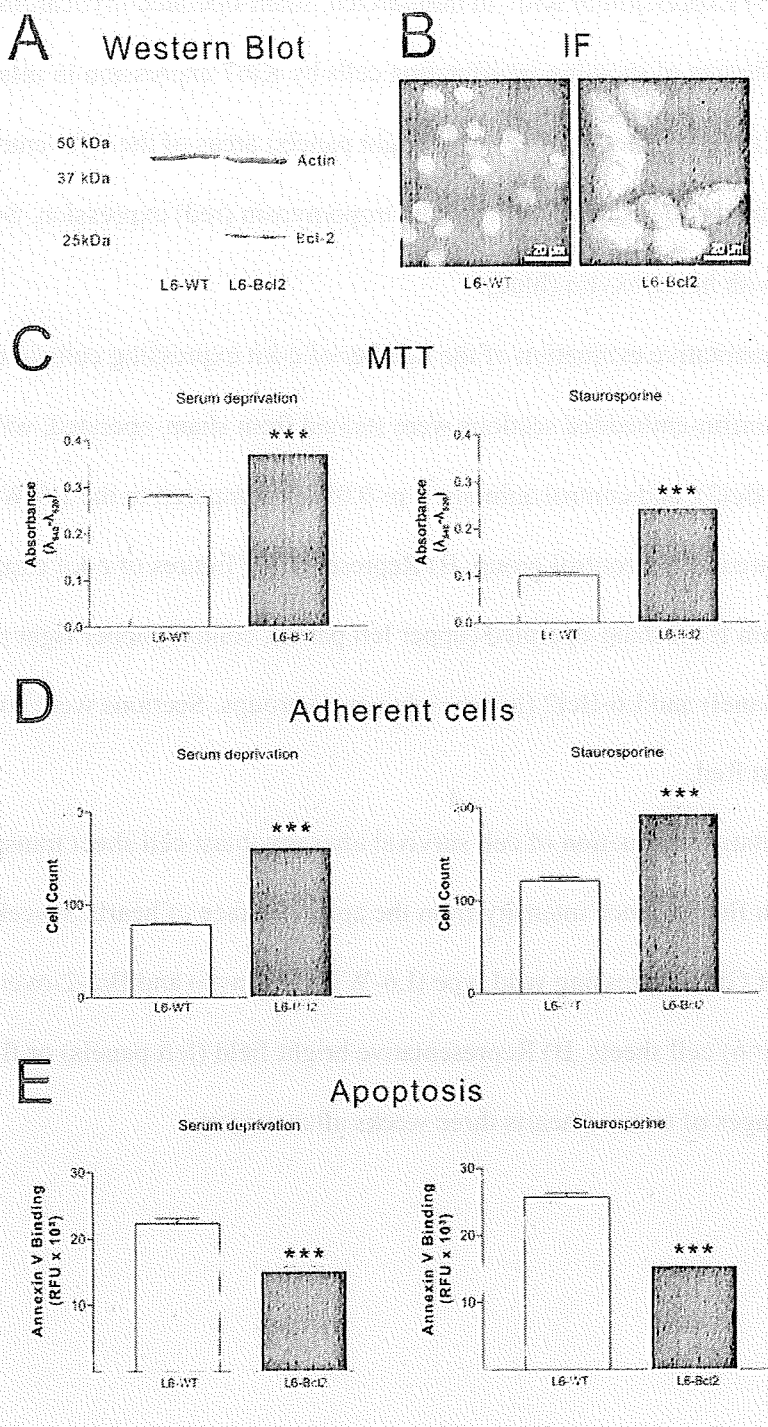
A
Western Blot
50 kDa
37 kDa
Actin
25kDa
Bcl-2
L6-WT
L6-Bcl2
B
IF
L6-WT
L6-Bcl2
C
MTT
Serum deprivation
Staurosporine
Absorbance
***
L6-WT
L6-Bcl2
D
Adherent cells
Serum deprivation
Staurosporine
Cell Count
***
L6-WT
L6-Bcl2
E
Apoptosis
Serum deprivation
Staurosporine
Annexin V Binding
(RFU x 10³)
***
L6-WT
L6-Bcl2

Figure 1:

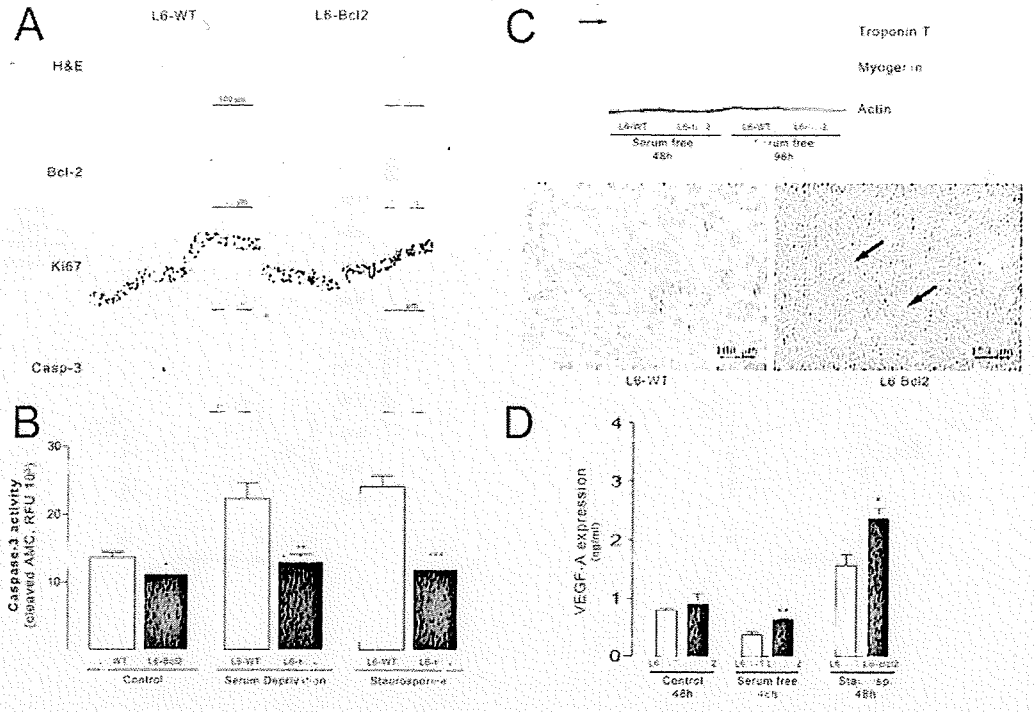
A
L6-WT
L6-Bcl2
H&E
Bcl-2
Ki67
Casp-3
C
Troponin T
Myogenin
Actin
Serum free
48h
96h
L6-WT
L6 Bcl2
B
Caspase-3 activity
(cleaved AMC, RFU 10³)
30
20
10
Control
Serum Deprivation
Staurosporine
D
VEGF-A expression
(ng/ml)
4
3
2
1
0
Control
48h
Serum free
48h

Figure 2:

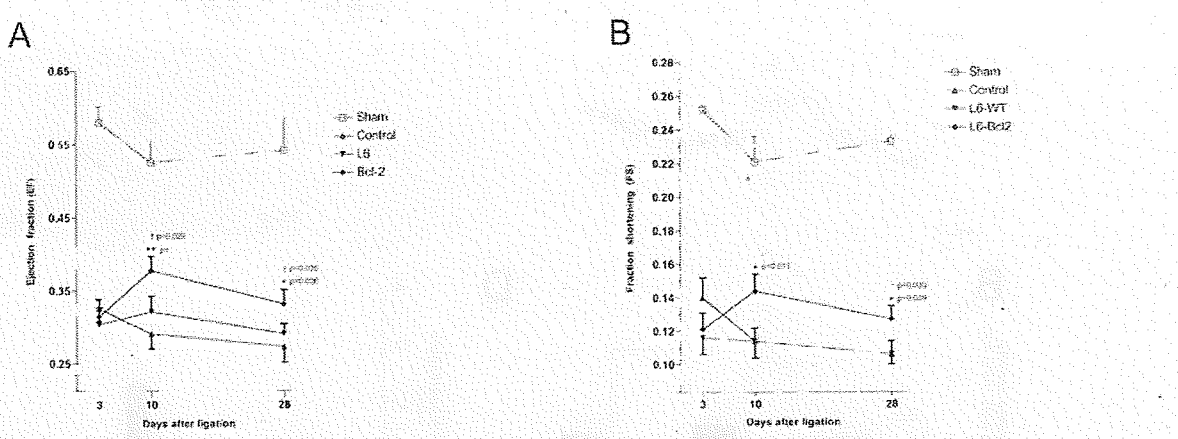
A
B
Sham
Control
L6
Bcl-2
L6-WT
L6-Bcl2
Ejection fraction (EF)
Fraction shortening (FS)
Days after ligation
3
10
28

Figure 3:

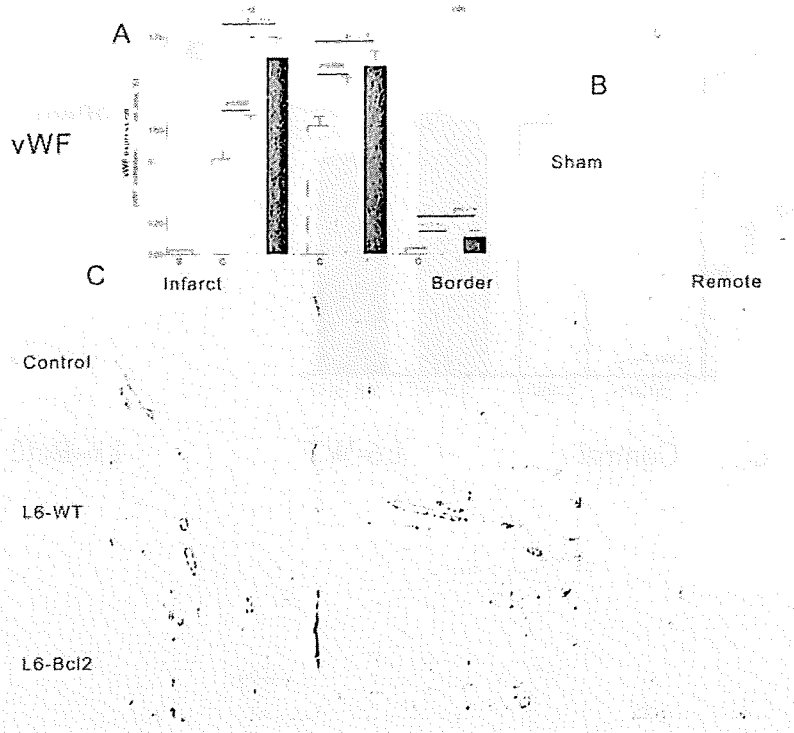

Figure 4:

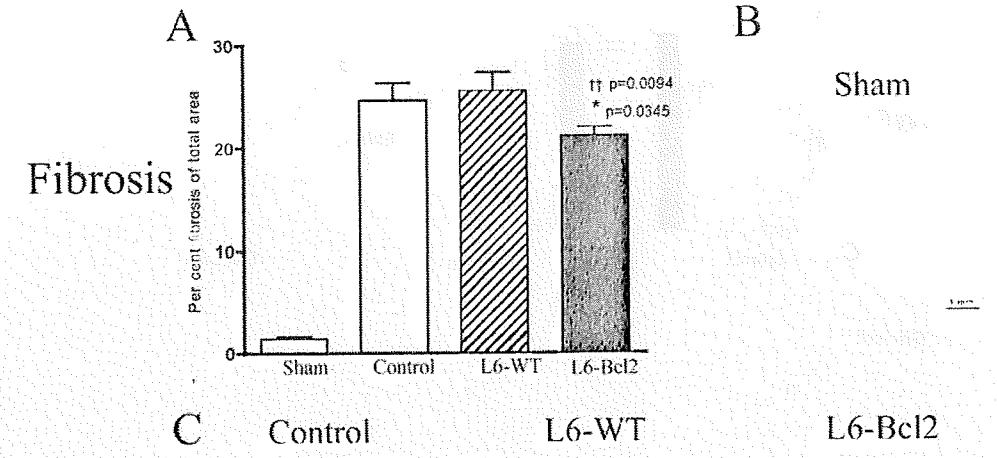
A
B
Sham
Fibrosis
Per cent fibrosis of total area
30
20
10
0
†† p=0.0094
* p=0.0345
Sham
Control
L6-WT
L6-Bcl2
C
Control
L6-WT
L6-Bcl2

Figure 5:

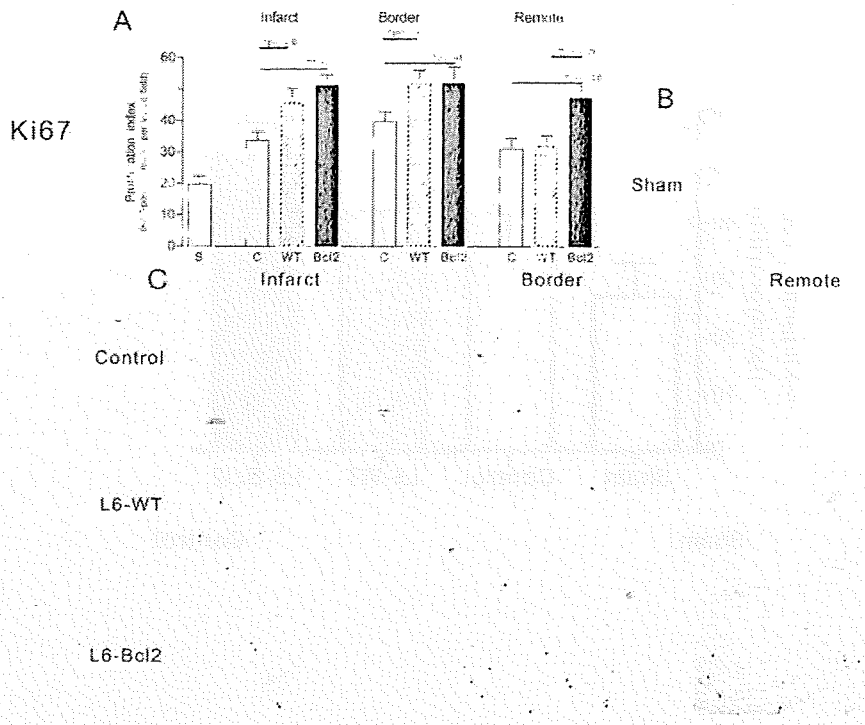
A
Infarct
Border
Remote
Ki67
B
Sham
S
C
WT
Bcl2
C
WT
Bcl2
C
WT
Bcl2
C
Infarct
Border
Remote
Control
L6-WT
L6-Bcl2

Figure 6:

A

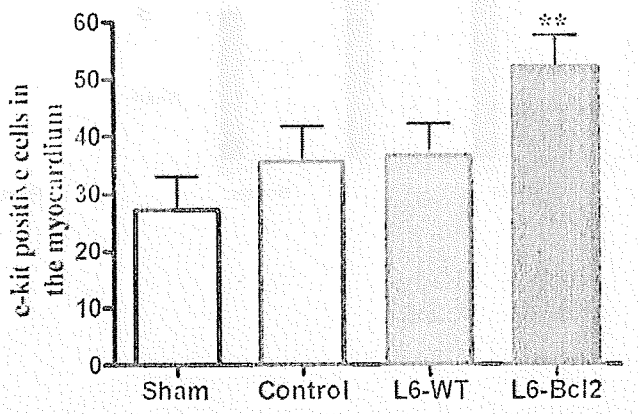
c-kit positive cells in the myocardium
60
50
40
30
20
10
0
**
Sham
Control
L6-WT
L6-Bcl2

B

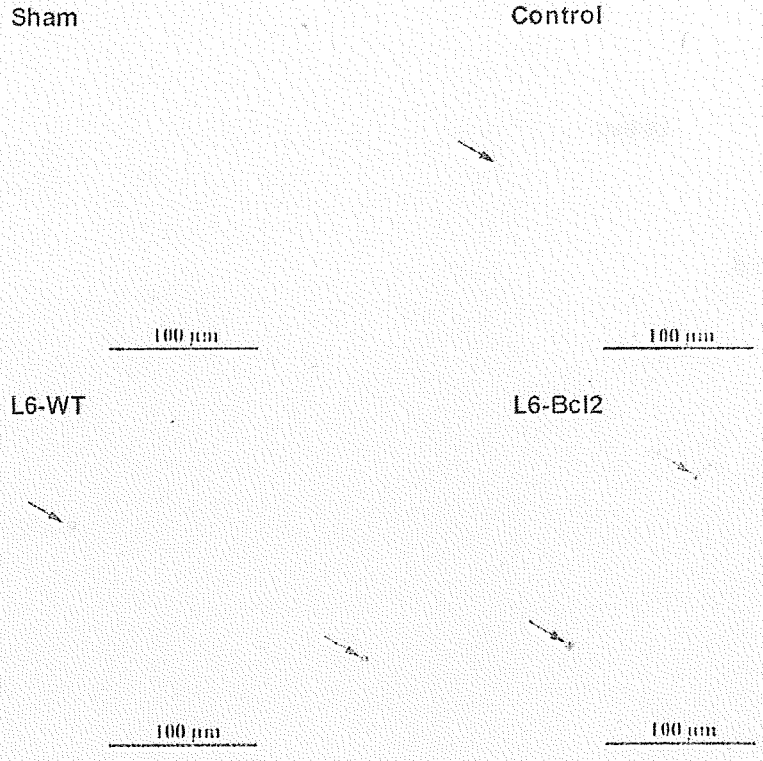
Sham
Control
100 μm
100 μm
L6-WT
L6-Bcl2
100 μm
100 μm

Figure 7:

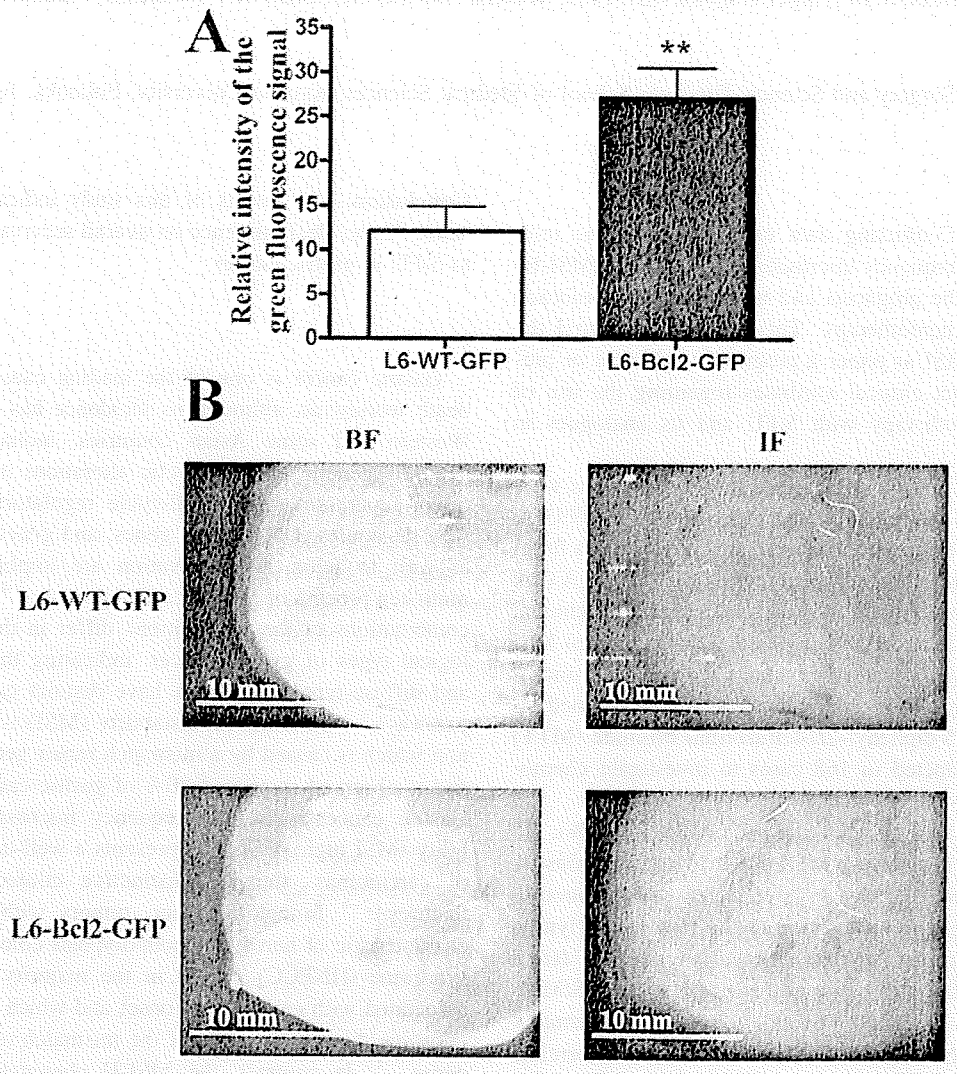
A
Relative intensity of the green fluorescence signal
35
30
25
20
15
10
5
0
**
L6-WT-GFP
L6-Bcl2-GFP
B
BF
IF
L6-WT-GFP
L6-Bcl2-GFP
10 mm
10 mm
10 mm
10 mm

Figure 8:

Ann Surg Oncol (2009) 16:2510–2515
DOI 10.1245/s10434-009-0580-8

Annals of
SURGICAL ONCOLOGY
OFFICIAL JOURNAL OF THE SOCIETY OF SURGICAL ONCOLOGY

ORIGINAL ARTICLE – GASTROINTESTINAL ONCOLOGY

Chemosensitivity and Survival in Gastric Cancer Patients with Microsatellite Instability

Eiji Oki, MD, PhD, Yoshihiro Kakeji, MD, PhD, Yan Zhao, MD, PhD, Rintaro Yoshida, MD, Koji Ando, MD, Takanobu Masuda, MD, Kippei Ohgaki, MD, PhD, Masaru Morita, MD, PhD, and Yoshihiko Maehara, MD, PhD, FACS

Department of Surgery and Science, Graduate School of Medical Sciences, Kyushu University, Fukuoka, Japan

ABSTRACT

Introduction. Conflicting data exist regarding the relevance of high-frequency microsatellite instability (MSI-H) for predicting the prognosis and benefits of 5-fluorouracil (5-FU)-based chemotherapy. This study investigated the usefulness of MSI as either a prognostic indicator or predictor of distinct clinical attributes regarding the use of adjuvant chemotherapy with 5-FU and its analogues in gastric cancer.

Materials and methods. Data and tumor specimens were collected from 240 gastric cancer patients from 1993 to 2002. Five microsatellite loci were analyzed using a high-intensity microsatellite analysis reported previously. A Cox proportional hazard model was used to compare the clinical data and survival as well as any associations between MSI and 5-FU treatment status of patients with MSI or microsatellite stability (MSS) gastric cancers. A 3-(4,5-dimethyl-2-thiazolyl) -2,5-diphenyl-2*H*-tetrazolium bromide (MTT) assay was conducted in 168 cases to investigate chemosensitivity to 5-FU.

Results. This analysis identified 22 MSI-H (9.4%), 25 MSI-L (10.7%), and 193 MSS (79.9%) tumors. Gastric cancer with MSI-H tended to have increased likelihood to show higher age, antral location of the tumor, and lymph vessel involvement ($P < 0.05$). Univariate analyses failed to show any difference between the MSI-H and MSS/MSI-L groups with respect to overall survival. Furthermore, survival after the administration of 5-FU did not correlate with MSI status, and MSI was not associated with 5-FU sensitivity by MTT assay.

Conclusion. The results of this study indicate that MSI status has no clear influence on overall survival or response to 5-FU in gastric cancer.

© Society of Surgical Oncology 2009

First Received: 6 March 2009;
Published Online: 30 June 2009

E. Oki, MD, PhD
e-mail: okieiji@surg2.med.kyushu-u.ac.jp

Gastric cancer is one of the leading causes of cancer death worldwide, although its incidence has decreased in Western and some Asian countries, including Japan.[1] Multiple genetic and epigenetic alterations in oncogenes, tumor-suppressor genes, cell-cycle regulators, cell adhesion molecules, DNA repair genes, and genetic instability as well as telomerase activation are implicated in the multistep process of gastric carcinogenesis.[2–4] The specific combinations of these alterations differ in the two histological types of gastric cancer, indicating that intestinal- and diffuse-type carcinomas have distinct carcinogenetic pathways.[2] Microsatellite instability (MSI) is a phenomenon which is caused by a mismatch repair gene deficiency and is observed in around 20% of gastric cancer patients. Gastric cancer with high-frequency microsatellite instability (MSI high; MSI-H) represents a well-defined subset of carcinomas, showing distinctive clinicopathological features.[1,5–8] In colon cancer, tumors with MSI-H are characteristic of hereditary nonpolyposis colorectal cancer syndrome (HNPCC) which, in the majority of cases, is associated with early age at onset and which is caused by germline mutations in one of the mismatch repair (MMR) genes.[9–12] In contrast, the MSI-H phenotype in gastric cancer is predominantly caused by epigenetic hypermethylation of the *hMLH1* as MMR gene rather than germline mutations in one of the MMR genes.[13–15] Hypermethylation of the promoter of the *hMLH1* gene occurs in more than 30% of human gastric cancer tissues.[13,16,17] Thus MSI in gastric cancer is frequent enough not to be ignored. Not only genetic factors but also dietary intake, cigarette smoking, and alcohol consumption may influence the

development of hMLH1-methylated gastric cancer.[16] MSI-H and microsatellite stable (MSS)/MSI-L gastric cancer differ in some pathological and clinical findings.[1,5,18] Many studies found a better prognosis of MSI-H tumors in comparison with MSI-Land MSS tumors with respect to overall and disease-free survival.[1,5,19] However, other studies found no influence of MSI on survival.[20–22] The mechanism by which MSI may influence clinical outcome is unknown in gastric cancer.

Currently, tumor stage is the most important predictor of prognosis for gastric cancer. A recent pivotal Japanese trial showed that systemic adjuvant chemotherapy using an oral 5-FU derivative improved survival time for stage II and III gastric cancer.[23] In the same manner as for gastric cancer, adjuvant chemotherapy improved the survival of stage II and III colon cancer. However, some studies found that MSI-H tumors may be resistant to 5-FU.[24,25] In contrast, others found a better chemosensitivity in MSI-H tumors.[25–27] However, these findings remain controversial. So far, no-one has shown any clear results in regard to whether MSI is a prognostic or predictive factor for 5-FU sensitivity in gastric cancer. This study was therefore a retrospective study of unselected patients with gastric cancer, irrespective of age at diagnosis or tumor stage, to identify tumor MSI status and analyze its relationship with overall survival and chemosensitivity.

PATIENTS AND METHODS

Tissue Samples

Primary gastric carcinoma tissues and corresponding normal mucosa were obtained from 240 Japanese patients who underwent surgery in the Department of Surgery II at Kyushu University Hospital between 1993 and 2000. No patient had received chemotherapy before surgery. Informed consent was obtained from each patient prior to tissue acquisition, and the study was approved by the ethical committee of Kyushu University. All the tumors, examined microscopically by pathologists, were diagnosed as adenocarcinoma and classified according to the criteria of the Japanese Research Society for Gastric Cancer. The cancer tissues and the well-separated normal gastric mucosa obtained from the gastrectomies were immediately cut into two pieces. Half of the specimen was kept in liquid nitrogen for DNA extraction, and the another half was immediately put into medium (Minimal Essential Medium; MEM) for chemosensitivity tests. The genomic DNA was prepared by proteinase K digestion and phenol–chloroform extraction, which was then followed by ethanol precipitation. In all cases, the histopathological type of the tumors was determined to be adenocarcinoma.

Microsatellite Instability Analysis

MSI was analyzed in this study using a DNA sequencer with five microsatellite markers. The oligonucleotide primers were synthesized and then purified by high-performance liquid chromatography (HPLC). The sequences of the primers for polymerase chain reaction (PCR) were: D2S123-5′; 5′-AAACAGGATGCCTGCCTTTA, D2S123-3′; 5′-GGACTTTCCACCTATGGGAC, D5S107-5′; 5′-GGCATCAACTTGAACAGCAT, D5S107-3′; 5′-GATCCACTTTAACCCAAATAC, D10S197-5′; 5′-ACCACTGCACTTCAGGTGAC, D10S197-3′; 5′-GTGATACTGTCCTCAGGTCTCC, D11S904-5′; 5′-ATGACAAGCAATCCTTGAGC, D11S904-3′; 5′-CTGTGTTATATCCCTAAAGTGTGA; D13S175-5′; 5′-TGCATCACCTCACATAGGTTA, D13S175-3′; 5′-TATTGGATACTTGAATCTGCTG. The PCR reactions using genomic DNA were performed using a TAKARA GeneAmp PCR Reagent Kit and were run in a Perkin-Elmer GeneAmp PCR system 9700 (Norwalk, CT). The thermal conditions of the system were as follows: one cycle at 95°C for 4 min; 35 cycles at 95°C for 0.5 min, 55°C for 0.5 min, and 72°C for 0.5 min; and one cycle at 72°C for 10 min. The DNA derived from the cancer tissues were amplified with ROX-labeled 5′ primer and cold 3′ primer, whereas the DNA from the normal tissues was amplified with HEX-labeled 5′ primer and cold 3′ primer. The running condition of the Perkin-Elmer Genetic Analyzer 310 (Norwalk, CT) was described previously.[27] The data were processed by the ABI software GeneScan. An alteration in the length of a microsatellite PCR fragment obtained from a cancerous tissue specimen was defined as MSI positivity. The detailed determination method was previously reported.[12,28] MSI status was classified as follows: high frequency of microsatellite instability (MSI-H) when MSI was demonstrated in two or more of five analyzed markers, low frequency of microsatellite instability (MSI-L) when MSI was demonstrated in one out of five analyzed markers, and microsatellite stability (MSS) when no positive MSI were detected in any of the loci.

Chemosensitivity Test

One hundred and sixty-eight patient specimens underwent an in vitro chemosensitivity test. The succinate dehydrogenase inhibition (SDI) test was conducted as previously described by Takeuchi et al.[29,30] Cell viability was estimated based on succinate dehydrogenase (SD) activity, and was determined using 3-(4,5-dimethyl-2-thiazolyl) -2,5-diphenyl-2*H*-tetrazolium bromide (MTT).

Statistical Methods

Statistical significance was determined using Student's *t*-test and the chi-square test with Yates's correlation factor, and was also confirmed via a two-tailed Fisher exact test. A difference was considered significant when the *P*-value was less than 0.05.

RESULTS

Correlations Between MSI Status and Clinicopathological Factors in Gastric Cancer

Screening identified 240 patients with gastric cancers for whom pathological material and follow-up data were available. Table 1 shows 22 MSI-H (9.4%), 25 MSI-L (10.7%), and 193 MSS (79.9%) tumors. In many previous reports, MSI status was categorized into two groups, including MSI-H and MSS/MSI-L, since MSI-L tumors demonstrate very similar clinicopathological features to those of MSS tumors.[24–26] In our past reports, MSI was classified into type A and type B MSI.[12,31–34] However, a classification of MSI-L and MSI-H was used in this article simply to discuss the pathological characteristics. Furthermore, in the same way as noted in other previous reports, MSS and MSI-L were categorized in the same group as MSS/MSI-L. MSI-H was associated with higher age ($P < 0.05$), antral location of the tumor ($P < 0.05$), and lymph vessel involvement ($P < 0.05$); however, MSI-H was not associated with the intestinal type according to Lauren classification, depth of invasion or tumor stage (Table 2).

MSI Status and Prognosis in Gastric Cancer

The median follow-up of all patients was 983 ± 861 days and within the study period, 64 patients (28.2%) died. Adjuvant chemotherapy was performed for 76/240 (31.7%) patients. A Cox regression model for a univariate analysis was used to assess the effect of MSI status on survival. This analysis failed to show any difference between the MSI-H and MSS/MSI-L groups with respect to overall survival (Fig. 1).

TABLE 1 Frequency of microsatellite instability of gastric cancer

MSI status	Incidence (%)
MSS	193 (79.9%)
MSI-L	25 (10.7%)
MSI-H	22 (9.4%)

TABLE 2 Clinicopathological features and microsatellite instability of gastric cancer

Variable	MSS/MSI-L ($n = 218$)	MSI-H ($n = 22$)	*P*-value
Gender			
Male	123	6	N.S.
Female	69	16	
Age	63.3	67.8	<0.05
Histology[a]			
Intestinal	84	11	N.S.
Diffused	113	11	
Depth of invasion			
T1, T2	95	13	N.S.
T3, T4	98	9	
Histological lymph node metastasis			
Negative	54	10	N.S.
Positive	139	12	
Lymph vessel involvement			
ly (–)[b]	59	1	<0.05
ly (+)[c]	134	21	
Vascular involvement			
Negative	111	13	N.S.
Positive	82	9	
Location[d]			
E/U[e]	67	2	<0.05
M/L	125	20	
Stage			
I + II	86	12	N.S.
III + IV	107	10	

[a] Case for which the histological diagnosis could not be determined were excluded

[b] ly (–) No lymphatic invasion was observed

[c] ly (+) The lymphatic invasion was observed

[d] Case for which the location could not be determined were excluded

[e] The tumor location was expressed as followings; the esophagus (E), upper (U), middle (M), and lower (L)

MSI Status and Chemosensitivity in Gastric Cancer

The regimens in the 76 cases who received chemotherapy were as follows: tegafur/uracil in 27 cases, 5-FU bolus injection in 20 cases, doxifluridine in 11 cases, 1-hexylcarbamoyl-5-fluorouracil (HCFU) in 8 cases, tegafur in 6 cases, and tegafur/gimeracil/oteracil potassium in 4 cases. They are all derivatives of 5-fluorouracil.

A Cox regression model for a univariate analysis was used to assess the effect of MSI status on survival in the 76 patients who underwent adjuvant chemotherapy. We found a small difference between the patients who received adjuvant chemotherapy and those who did not receive any adjuvant chemotherapy, but it was not significant (Fig. 2a).

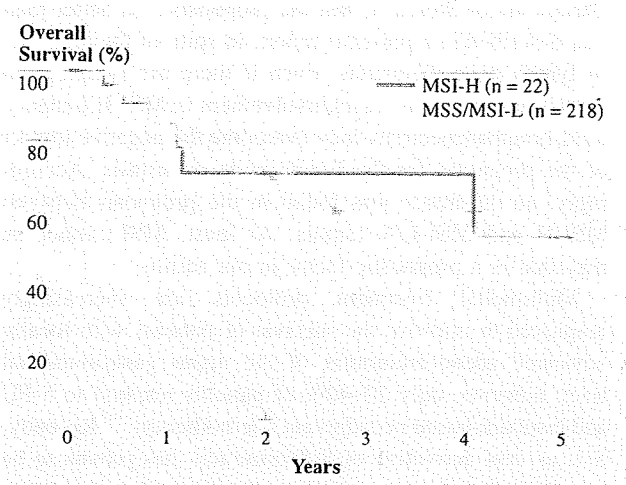

FIG. 1 Overall survival in all cases. The bold line is MSS and dotted line is MSI-H/L

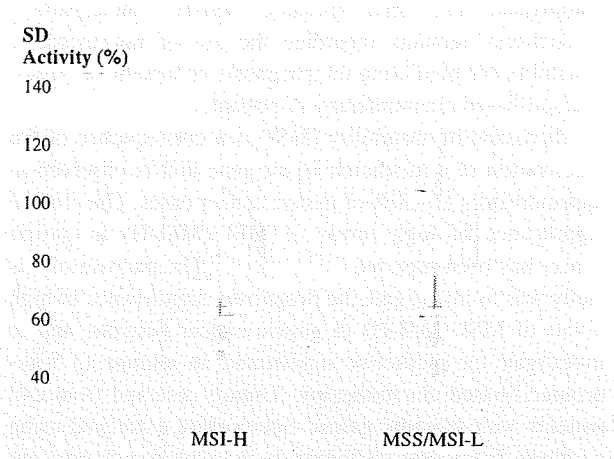

FIG. 3 In vitro chemosensitivity test using MTT assay. When the chemotherapeutic sensibilities of these patients were studied in an MTT assay, MSI was not associated with 5-FU sensitivity. Cell viability was estimated based on succinate dehydrogenase (SD) activity, and was determined using 3-(4,5-dimethyl-2-thiazolyl) -2,5-diphenyl-2H tetrazolium bromide (MTT)

Survival after administration of 5-FU or its derivatives did not correlate with MSI status (Fig. 2b). When the chemotherapeutic sensibilities of these patients were studied in an MTT assay in 168 patients, MSI was not associated with the 5-FU sensitivity (Fig. 3). The chemosensitivity test was repeated for the other chemotherapeutic agents, such as cisplatin (CDDP), adriamycin, and mitomycin; however, no difference was found among the patients regarding each MSI status group (data not shown).

DISCUSSION

Gastric cancer (GC) remains a leading cause of cancer mortality worldwide. Although the association between clinicopathological factors and MSI has been well investigated in colon cancer, their proportion and association with clinicopathological factors remain to be proven in gastric cancer. It is unclear whether MSI is a prognostic factor or a predictive factor in gastric cancer. The most important clinical findings concerning microsatellite instabilities is their effect on the prognosis of patients and chemosensitivity to 5-FU for adjuvant chemotherapy in colon cancer. There is improved survival in patients with non-microsatellite instability-high (MSI-L/N) tumors after 5-fluorouracil-based chemotherapy that does not extend to patients with microsatellite instability-high tumors (MSI-H).[24] Benatti et al. also reported that type of genomic instability could influence the prognosis of CRC, in particular in stages II and III, and 5-fluorouracil-based chemotherapy does not improve survival among MSI-H patients. Therefore, MSI is regarded as a predictive factor in colon cancer. However, the survival difference was influenced by the patients of hereditary nonpolyposis (HNPCC) colorectal cancer who were diagnosed at a younger age and less advanced in

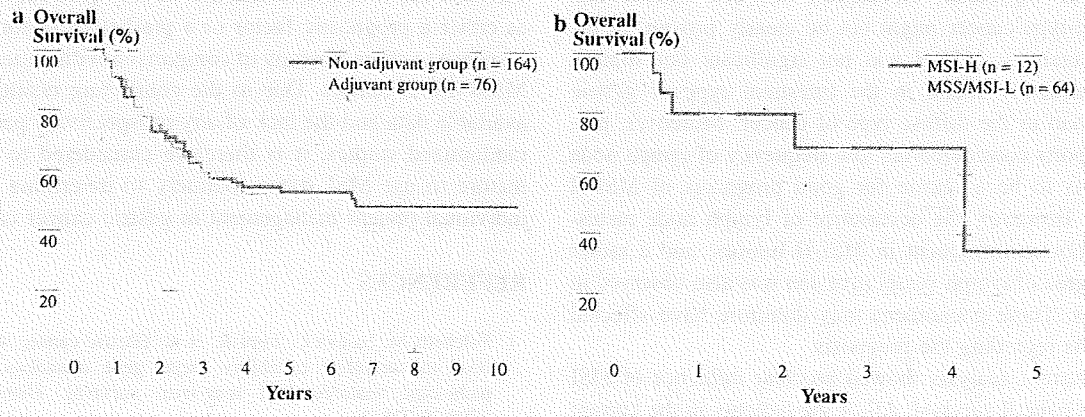

FIG. 2 **a** Overall survival in all cases following the use of adjuvant chemotherapy. The bold line is for the patients who received adjuvant chemotherapy and the dotted line is for the patients who did not received adjuvant chemotherapy. **b** Overall survival following the use of adjuvant chemotherapy. The bold line is for MSS and dotted line is for MSI-H/L